Chemotype-dependent Metabolic Response to Methyl Jasmonate Elicitation in *Artemisia annua*

Authors Wei Wu[1,2], Man Yuan[1,3], Qing Zhang[1], Yanming Zhu[3], Li Yong[3], Wei Wang[1], Yan Qi[1], Dianjing Guo[1]

Affiliations
[1] School of Life Sciences and the State Key Laboratory for Agrobiotechnology, The Chinese University of Hong Kong, HKSAR, China
[2] Plant Bioengineering Laboratory, Northeast Agricultural University, Harbin, China
[3] Changchun University of Chinese Medicine, Changchun, China

Key words
- *Artemisia annua* L.
- Asteraceae
- methyl jasmonate
- chemotype
- GC-MS
- real time RT-PCR

received August 11, 2010
revised Nov. 30, 2010
accepted Dec. 21, 2010

Bibliography
DOI http://dx.doi.org/10.1055/s-0030-1250744
Published online January 25, 2011
Planta Med 2011; 77: 1048–1053 © Georg Thieme Verlag KG Stuttgart · New York · ISSN 0032-0943

Correspondence
Dianjing Guo
School of Life Sciences and the State Key Laboratory for Agrobiotechnology
The Chinese University of Hong Kong
HKSAR
China
Phone: + 852 26 09 62 98
Fax: + 852 26 03 57 45
djguo@cuhk.edu.hk

Abstract

Considerable difference in artemisinin and its direct precursors, artemisinic acid and dihydroartemisinic acid, was detected between two chemotypes within the species *Artemisia annua (A. annua)*. These two chemotypes showed differential metabolic response to methyl jasmonate (MeJA) elicitation. Exogenous application of MeJA resulted in an accumulation of dihydroartemisinic acid and artemisinin in Type I plants. In Type II plants, however, artemisinic acid and artemisinin level decreased dramatically under MeJA elicitation. Squalene and other sesquiterpenes, (e.g., caryophyllene, germacrene D), were stimulated by MeJA in both chemotypes. The effect of MeJA elicitation was also studied at the transcription level. Real time RT-PCR analysis showed a coordinated activation of most artemisinin pathway genes by MeJA in Type I plants. The lack of change in cytochrome P450 reductase (CPR) transcript in Type I plants indicates that the rate-limiting enzymes in artemisinin biosynthesis have yet to be identified. Other chemotype-specific electron donor proteins likely exist in *A. annua* to meet the demand for P450-mediated reactions in MeJA-mediated cellular processes. In Type II plants, mRNA expression patterns of most pathway genes were consistent with the reduced artemisinin level. Intriguingly, the mRNA transcript of aldehyde dehydrogenase1 (ADHL1), an enzyme which catalyzes the oxidation of artemisinic and dihydroartemisinic aldehydes, was upregulated by MeJA. The differential metabolic response to MeJA suggests a chemotype-dependent metabolic flux control towards artemisinin and sterol production in the species *A. annua*.

Abbreviations

GC-MS: gas chromatography-mass spectrometry
RT-PCR: reverse transcription-polymerase chance reaction
CYP: cytochrome P-450
ROS: reactive oxygen species

Introduction

Artemisinin, a sesquiterpene lactone produced in *Artemisia annua*, has attracted considerable attention from researchers in recent years. Artemisinin and its derivatives form the fundament for artemisinin-based combination therapies (ACTs), which are the current treatment of choice for the deadly disease malaria. Artemisinin is also effective against several other parasites, e.g., *Schistosoma spp.* [1] and hepatitis B virus [2]. Lines of evidence also suggest that artemisinin can inhibit or delay the development of a variety of cancer cell lines, including human leukemia, breast cancer, colon, and small-cell lung carcinomas [3]. Given the low artemisinin concentration in *A. annua* (0.01–0.8% of dry weight [4]), a complete understanding of artemisinin biosynthesis and metabolism holds the key to improving artemisinin yield through metabolic engineering efforts.

The C5 building blocks of artemisinin can be derived from both mevalonate and nonmevalonate pathways [5]. The formation of amorpha-4,11-diene by amorpha- 4,11-diene synthase (ADS) is the first committed step, followed by the oxidation of amorpha-4,11-diene by the cytochrome P-450 CYP71AV1 to yield artemisinic alcohol [6,7] (**Fig. 1**). CYP71AV1 is also capable of oxidizing artemisinic alcohol into artemisinic acid via artemisinic aldehyde. Although some early evidence suggests that artemisinic acid is an intermediate in the artemisinin pathway, artemisinin appears

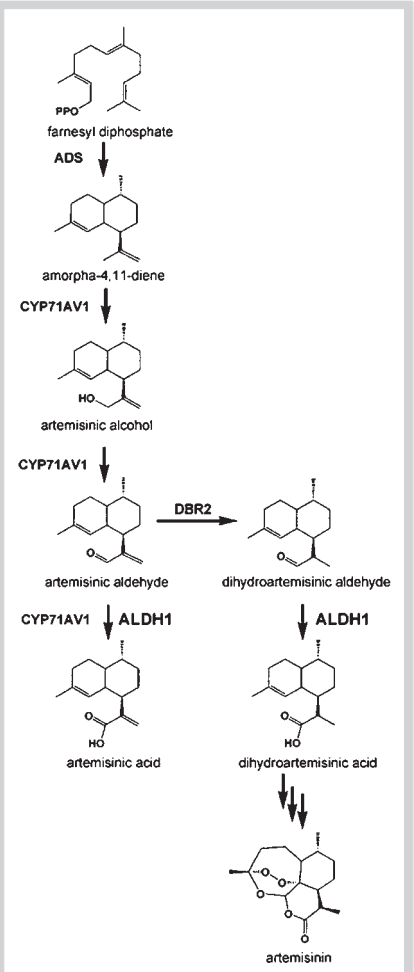

Fig. 1 A proposed biosynthetic pathway of artemisinin in *A. annua* (adapted from Teoh et al. [12]).

to be derived from dihydroartemisinic acid in a series of photooxygenic reactions [8,9]. Biochemical evidence of NAD/NADP-dependent oxidation of dihydroartemisinic aldehyde in extracts of *A. annua* [8,10] and the recent cloning of artemisinic aldehyde D11 double bond reductase (DBR2) provide strong evidence that dihydroartemisinic acid is formed via the oxidation of dihydroartemisinic aldehyde [11]. Most recently, the expression of an aldehyde dehydrogenase (ALDH1) cDNA in *E. coli* and the characterization of purified recombinant enzyme demonstrate that ALDH1 catalyses the NAD(P)-dependent oxidation of the putative artemisinin precursors, artemisinic and dihydroartemisinic aldehydes [12].

Jasmonates (JAs) are important plant hormones [13,14] and their ability to modulate gene expression in plant defense responses has been well documented [15]. As potent elicitors or signaling agents, JAs have also been suggested as mediators of secondary product accumulation [16]. The exogenous application of JAs, as well as their conjugated compounds such as methyl jasmonate (MeJA), can stimulate secondary metabolites production in a variety of plant species [17]. A previous study has shown that artemisinin production can be enhanced by different elicitors in *A. annua* cell cultures and hairy root cultures [18]. However, to our knowledge, the effect of MeJA elicitation on secondary metabolites in different *A. annua* chemotypes has not yet been investigated. The correlation between the expression pattern of pathway genes and terpenoids profile in response to MeJA has also yet to be established. The main objectives of this study are therefore to evaluate the effect of MeJA elicitation on terpenoids profile, especially sesquiterpenes, in different *A. annua* chemotypes. Real time RT-PCR analysis was conducted to correlate the accumulation of sesquiterpene metabolites under MeJA elicitation with transcription rates of the respective pathway genes.

Materials and Methods

Plant materials and MeJA treatment

Two *Artemisia annua* L. cultivars were used in all experiments. The seed samples (#YY0801 and #SH0802) are deposited in the Hong Kong Herbarium. Seeds of chemotype I (#YY0801) were purchased from Youyang (Sichuang province, China) and seeds of Type II chemotype (#SH0802) were kindly provided by Prof. Chen Xiaoya at the Institute of Plant Physiology and Biochemistry, Chinese Academy of Sciences. Seeds were germinated and grown in soil under controlled conditions (12 h day/12 h night regimen at 22 °C) until the seedlings formed 8 leaves. 100 µM MeJA was then sprayed onto the leaf surface. Mock solution was applied to control plants at the same developmental stage. Leaf samples were collected at 0, 6, 12, and 24 hours respectively. For each group, 5 individual plants were used as biological repeats. Pooled leaf samples were frozen in liquid nitrogen and stored at −80 °C for further analysis.

Chemicals and GC-MS analysis

Methyl jasmonate was purchased from Aldrich. Camphor (≥ 96%) and phytol (≥ 90%) were purchased from Fluka. Caryophyllene (0.902 g/mL), germacrene D (≥ 96%), and squalene (≥ 98%) were purchased from Sigma Chemical Co. Artemisinic acid (≥ 95%) was purchased from the Chinese Authenticating Institute of Material Medical and Biological Products (Peking, China). Dihydroartemisinic acid (≥ 95%), dihydro-epi-deoxyarteannuin B (≥ 95%), and deoxyqinghaosu (≥ 93%) were gifts from the Natural Product Laboratory of the College of Pharmacy, Jilin University (Jilin, China).

For metabolite analysis, frozen tissues were first lyophilized. Thirty mg dry material were accurately weighed and extracted twice with a total of 2 mL dichloromethane containing 2 µg · mL^{-1} cis-nerolidol as the internal standard. Samples were then sonicated on ice for 30 min and centrifuged at 2000 rpm for 2 minutes. The supernatant was collected, dried and redissolved in 0.5 mL dichloromethane for GC-MS analysis.

GC-MS analysis was performed on HP 5890 series gas chromatograph and HP 5975 mass detector (70 eV), equipped with a capillary HP-5MS (95% dimethylpolysilane, 30 m × 0.25 mm i.d., film thickness 0.25 µm). The carrier gas was He (1 mL/min). The inlet temperature and detector temperature were 250 °C and 290 °C, respectively. The oven was programmed at: 2 min 80 °C, 80 °C to 235 °C at 5 °C per min, 235 °C to 280 °C at 25 °C per min, and final time of 5 min.

Data preprocessing and PCA analysis

Data acquisition and the preprocessing procedure were designed to extract the maximum amount of reliable information from the chromatograms. The compounds were identified by comparison of retention time and fragments with standards, and by matching compound fragment patterns with those in the NIST library scoring above 700. The software tools Metalign [19] and XCMS [20] were used for automated baseline correction and alignment of all the extracted mass peaks across samples. After automatic

peak extraction and alignment of samples, metabolites were predicted by retention time and *m/z* value. The retention time shift was taken into account and was corrected by calculating the median retention time and the deviation for each sample. Local polynomial regression was used to fit the change from the deviation. A data matrix was formed in which columns represented the samples and rows represent the *m/z* values.

Real time RT-PCR analysis

Total RNA was extracted from the whole seedlings of mock-treated control and MeJA-treated *A. annua* plants using RNeasy Plant Mini Kit (Qiagen). First-strand cDNA was synthesized from 1.5 µg total RNA using super script II Kit (Invitrogen) with Oligo (dT)12–18 mer. Quantitative real-time RT-PCR was carried out with the IQ5 Multicolor Real-time PCR Detection System (Bio-Rad) using the 0.5X iQ™ SYBR Green Supermix (Bio-Rad) and gene-specific primer. The cycling conditions were: 10 min 95 °C, followed by 40 cycles of 30 s 95 °C, 30 s 60 °C, 30 s 72 °C. Experiments were performed in three biological replicates and three technical replicates. Gene expression levels of genes were calculated relative to the mock treatment with normalization to ACTIN 2.

The forward and reverse gene specific primers are listed in **Table 1**.

Table 1 The forward and reverse gene specific primers.

Gene	Forward primer 5′-3′ sequence	Reverse primer 5′-3′ sequence
ADS	GAATGGGCTGTCTCTGCACCTCC	GGTTTGGGCATACTCCTCATTGACA
CYP71A	GGAATTGAGGAAAGCATTGAACGG	CAGAACCAAGGGTAGTGGAGGGTG
CPR	CCATTTCTTCTTCCCCAAGGTTTG	GTCATAGGCACGGCATTGTTCATC
ABRS	GGCATAAATGACAGAACGGACGAAT	CGATTGCAGGGGAGATTCTAAGACC
ALDH	CCTTGGAATGGTCCTGCCTTCA	GTTAACCACATTAATCACGC
ACTIN2	CCATCCTTCGTTTGGACTTGGC	CAATTTCCCGCTCTGCTGTGGT

Results and Discussion

Fig. 2 shows typical total ion chromatographs obtained from leaf tissue of Type I and Type II plants. Although virtually all of the observed variations in the terpenoids profile were quantitative rather than qualitative, considerable differences in the concentration of artemisinin, artemisinic acid, and dihydroartemisinic acid were found between these two chemotypes. Much high-

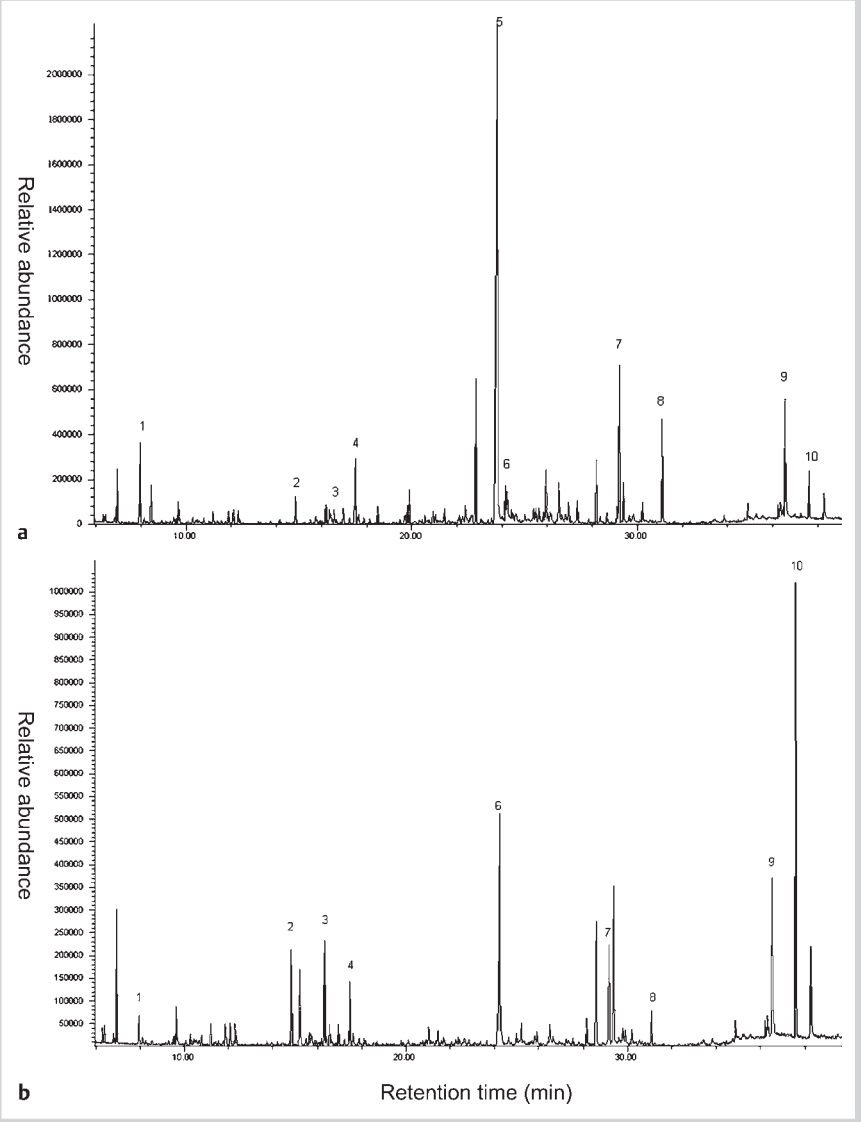

Fig. 2 Typical total ion chromatographs obtained from leaf tissue of *Artemisia annua* Type I (**a**) and Type II (**b**) plants. Identified compounds were selectively labeled. (**1**) Camphor $C_{10}H_{16}O$, (**2**) caryophyllene $C_{15}H_{24}$, (**3**) germacrene D $C_{15}H_{24}$, (**4**) farnesol isomer $C_{15}H_{26}O$, (**5**) dihydroartemisinic acid, $C_{15}H_{24}O_2$, (**6**) artemisinic acid, $C_{15}H_{22}O_2$, (**7**) artemisinin $C_{15}H_{22}O_5$, (**8**) dihydroartemisinin, 3-deoxy, $C_{15}H_{24}O_4$, (**9**) glyceryl monostearate, $C_{21}H_{42}O_4$, (10) squalene.

Table 2 Differential metabolic response to MeJA elicitation in two chemotypes.

Metabolite	Type I Relative amounts* Treated/Control (Fold change)	Type II Relative amounts* Treated/Control (Fold change)
Phytol	1.53 ± 0.17/0.52 ± 0.04 (2.94)	2.11 ± 0.19/0.58 ± 0.08 (3.64)
Squalene	2.04 ± 0.29/0.52 ± 0.07 (4.01)	6.52 ± 0.53/0.56 ± 0.07 (11.64)
Caryophyllene	1.57 ± 0.21/0.51 ± 0.11 (3.08)	1.93 ± 0.21/0.56 ± 0.04 (3.45)
Germacrene	1.07 ± 0.17/0.31 ± 0.05 (3.45)	2.81 ± 0.22/0.92 ± 0.12 (3.05)
Dihydroartemisinic acid	23.57 ± 2.12/12.51 ± 1.09 (1.88)	T
Dihydro-epi-deoxy-arteannuin B	1.54 ± 0.23/1.06 ± 0.17 (1.45)	T
Deoxyqinghaosu	1.31 ± 0.18/1.21 ± 0.13 (1.08)	T
Artemisinin	4.53 ± 0.61/3.07 ± 0.63 (1.48)	1.25 ± 0.13/1.97 ± 0.21 (0.63)
Dihydroartemisinin, 3-deoxy	3.55 ± 0.27/2.51 ± 0.32 (1.41)	T
Glyceryl monostearate	2.23 ± 0.21/2.11 ± 0.19 (1.06)	2.72 ± 0.31/2.70 ± 0.23 (1.00)
Artemisinin B	0.81 ± 0.09/0.53 ± 0.08 (+ 1.52)	1.86 ± 0.15/2.39 ± 0.02 (0.78)
Artemisinic acid	T	7.82 ± 0.67/16.65 ± 1.59 (0.47)
1-Eicosanol	0.59 ± 0.67/0.46 ± 0.38 (1.28)	1.91 ± 0.16/1.83 ± 0.23 (1.04)

* Ratio of individual metabolite peak area over that of the internal standard cis-nerolidol. Five *A. annua* plants at the 8-leaves stage were subjected to 100 µM MeJA treatment. Leaf samples were taken from 5 individual plants after 24 h treatment. T: only trace amount of metabolites were detected in both control and MeJA treated samples

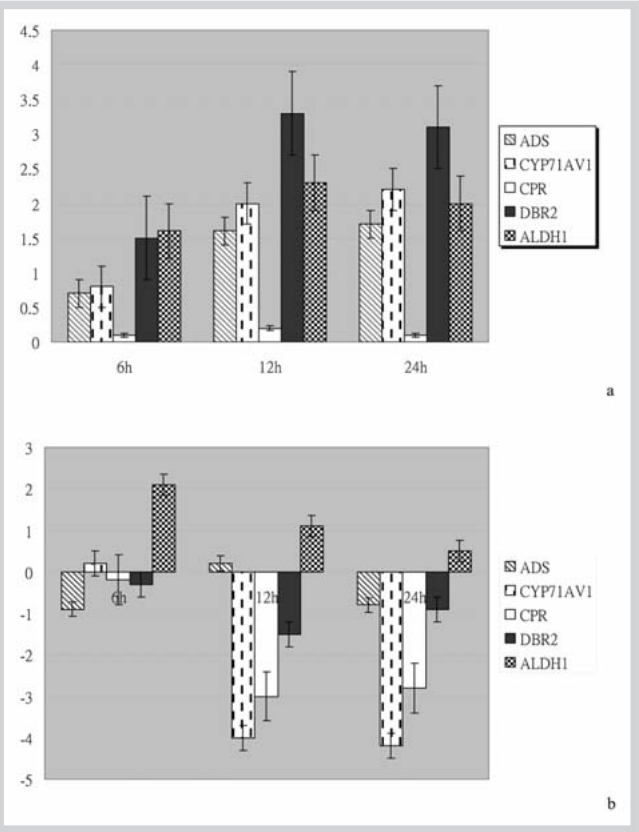

Fig. 3 Effects of MeJA elicitation on artemisinin pathway gene transcripts. **a**. Type I *A. annua*. **b**. Type II *A. annua*. X-axis: treatment time. Y-axis: $\log_2$ fold change of pathway gene transcript relative to transcript level at 0 h.

er levels of dihydroartemisinic acid and artemisinin were found in Type I plants. Conversely, notably lower levels of artemisinin and dihydroartemisinic acid but higher levels of artemisinic acid were detected in Type II plants. These two chemotypes, which were also reported earlier by Wallaart et al. [21], provide an ideal system for a comparative study aimed at obtaining a better understanding of artemisinin and terpenoid metabolism in *A. annua*.

To characterize the effect of MeJA elicitation on artemisinin production, a range of sesquiterpenoids was measured by GC/MS. These two chemotypes were found to be differentially regulated, and the chemotype-specific metabolic response to MeJA elicitation is illustrated in **Table 2**. In Type I plants, MeJA elicitation resulted in an accumulation of artemisinin and dihydroartemisinic acid, and the level of the latter increased by nearly two folds. In Type II plants, MeJA elicitation resulted in a reduced amount of artemisinin and artemisinic acid. Increased caryophyllene, germacrene D, and squalene levels were observed in both chemotypes ($p < 0.001$).

Terpenoids serve as both constitutive and inducible defense chemicals in many plant species. The exogenous application of MeJA may elicit a response similar to stress, and high levels of singlet oxygen are formed under such conditions. It is suggested that dihydroartemisinic acid may act as an antioxidant by quenching singlet oxygen, yielding artemisinin as a stable end-product in which the reactive oxygen is stored. By maintaining high levels of dihydroartemisinic acid, the plants may be protected from injury caused by a high concentration of singlet oxygen. MeJA has been suggested to promote (E)-beta-caryophylle production in rice [22]. Germacrenes are typically produced in a number of plant species for their antimicrobial and insecticidal properties, although they also play a role as insect pheromones. Further investigations are needed in order to elucidate the exact role of these sesquiterpenes in MeJA-mediated signaling events.

The squalene profile in MeJA-elicited *A. annua* plants increased significantly in both chemotypes ($p < 0.001$). Squalene has been proposed to act as a quencher of singlet oxygen and prevents the corresponding lipid peroxidation resulting from MeJA in animal studies [23]. The function of induced squalene by MeJA elicitation in *A. annua* remains to be determined.

To elucidate the effect of MeJA on pathway gene expression and to determine if the change of the terpenoids profile is also reflected at the transcript level, the mRNA expression of selected key artemisinin pathway genes was examined by real time RT-PCR with or without MeJA elicitation. The real time RT-PCR analysis employed gene-specific primers, and actin2 was used as an internal control. The time course mRNA expression profiles for CYP71AV1, ADS, CPR, DBR2, and ALDH1 gene are illustrated in **Fig. 3**.

As shown, MeJA elicitation had dramatic effects on most of the pathway gene transcripts, although the effects were quite different in these two chemotypes. For Type I plants, most examined

genes showed a coordinated upregulation in response to MeJA elicitation, consistent with the observation that application of MeJA resulted in an increased amount of artemisinin. Interestingly, the CPR transcript remained unchanged in Type I plants, indicating that the rate-limiting enzymes for artemisinin biosynthesis remain to be identified. For Type II plants, most of the genes were downregulated at various time points. The exception was ALDH1, which was induced at 6 h after elicitation.

Farnesol diphosphate (FDP) is a key intermediate compound situated at the branching point of the terpenoid pathway leading to sesquiterpene, triterpene, squalene, and polyterpene biosynthesis. The formation of amorpha-4,11-diene from FDP by amorpha-4,11-diene synthase (ADS) is the first committed step in artemisinin biosynthesis, followed by oxidation of amorpha-4,11-diene by the cytochrome P-450 CYP71AV1 to yield artemisinic alcohol (**Fig. 1**). The ADS, CYP71AV1, DBR2, and ALDH1 transcripts were all induced in Type I plants at different time points following addition of MeJA. CYP71AV1 belongs to the family of cytochrome P450 monooxygenase enzymes (P450s), which are known to play key roles in a wide range of oxidative metabolic reactions in various organisms. Using *A. annua* CPR as a redox partner for CYP71AV1, Ro et al. have shown that CYP71AV1 could catalyze the conversion of amorphadiene to more oxygenated artemisinic acid in yeast [24]. Divergent CPR genes have been characterized in parsley (*Petroselinum crispum*), *Arabidopsis* [25,26], and poplar [19]. The results of previous studies suggest that the CPR genes in these plants are differentially regulated. Some genes are constitutively expressed while others are enhanced or repressed by environmental stress, such as UV light and pathogen infection. It is also likely that *A. annua* plants may deploy distinctive classes of CYP/CPRs to meet the reductive demand for P450-mediated reactions in MeJA-mediated cellular processes.

Similar to the concerted upregulation of both mRNA and metabolite observed after MeJA elicitation in Type I plants, mRNA patterns of most pathway genes in Type II plants were also consistent with the reduced artemisinin level. Intriguingly, ALDH1, whose gene product catalyzes the oxidation of artemisinic and dihydroartemisinic aldehydes, was upregulated by MeJA elicitation. ALDHs represent a protein superfamily of $NAD(P)^+$-dependent enzymes that oxidize a wide range of endogenous and exogenous aldehydes. The *Arabidopsis* genome contains 14 unique ALDH sequences encoding members of 9 ALDH families [27]. In *A. annua*, however, only a limited number of ALDH has been reported so far. It is reasonable to suppose that *A. annua* ALDH1 may encode an enzyme with broad substrate specificity that allows it to detoxify other induced aldehydes under MeJA treatment.

It is also noteworthy that alongside the reduction of artemisinin levels, dramatic accumulations of two other types of sesquiterpenes, caryophyllene and germacrene D, were observed in both chemotypes. Further investigations of the chemotype-specific response under MeJA elicitation are warranted in order to determine the regulatory machinery underlying artemisinin and other sesquiterpenes biosynthesis. MeJA clearly plays a complex role in controlling secondary metabolism, especially with regard to terpenoid metabolism. In the present study, we demonstrated that exogenous application of MeJA elicited differential metabolic responses in these two chemotypes. Although a generally good correlation between gene transcripts and metabolites was found in artemisinin biosynthesis, our findings also raise a number of interesting issues that have yet to be addressed. For example, do any other rate-limiting enzymes exist in an artemisinin biosynthesis pathway? Does ALDH1 also function in cellular processes other than artemisinin biosynthesis? These questions deserve further investigation.

Acknowledgements

This work was funded by Research Grants Council of Hong Kong (grant no. CUHK4603/06M). We would also like to thank Dr. David Wilmshurst, CUHK's Academic Editor, for commenting on a draft of this paper.

References

1 *Xiao S.* Development of antischistosomal drugs in China, with particular consideration to praziquantel and the artemisinins. Acta Trop 2005; 96: 153–167
2 *Romero MR, Efferth T, Serrano MA, Castaño B, Macias RIR, Briz O, Marin JJG.* Effect of artemisinin/artesunate as inhibitors of hepatitis B virus production in an "*in vitro*" replicative system. Antiviral Res 2005; 68: 75–83
3 *Efferth T.* Molecular pharmacology and pharmacogenomics of artemisinin and its derivatives in cancer cells. Curr Drug Targets 2006; 7: 407–421
4 *Abdin MZ, Israr M, Rehman RU, Jain SK.* Artemisinin, a novel antimalarial drug: biochemical and molecular approaches for enhanced production. Planta Med 2003; 69: 289–299
5 *Towler MJ, Weathers PJ.* Evidence of artemisinin production from IPP stemming from both the mevalonate and the nonmevalonate pathways. Plant Cell Rep 2007; 26: 2129–2136
6 *Ro D, Ehlting J, Douglas CJ.* Cloning, functional expression, and subcellular localization of multiple NADPH-cytochrome P450 reductases from hybrid poplar. Plant Physiol 2002; 130: 1837–1851
7 *Teoh KH, Polichuk DR, Reed DW, Nowak G, Covello PS. Artemisia annua* L. (Asteraceae) trichome-specific cDNAs reveal CYP71AV1, a cytochrome P450 with a key role in the biosynthesis of the antimalarial sesquiterpene lactone artemisinin. FEBS Lett 2006; 580: 1411–1416
8 *Brown GD, Sy L. In vivo* transformations of dihydroartemisinic acid in *Artemisia annua* plants. Tetrahedron 2004; 60: 1139–1159
9 *Smith CA, Want EJ, O'Maille G, Abagyan R, Siuzdak G.* XCMS: processing mass spectrometry data for metabolite profiling using nonlinear peak alignment, matching, and identification. Anal Chem 2006; 78: 779–787
10 *Bertea CM, Freije JR, van der Woude H, Verstappen FW, Perk L, Marquez V, De Kraker JW, Posthumus MA, Jansen BJ, de Groot A, Franssen MC, Bouwmeester HJ.* Identification of intermediates and enzymes involved in the early steps of artemisinin biosynthesis in *Artemisia annua*. Planta Med 2005; 71: 40–47
11 *Zhang Y, Teoh KH, Read DW, Maes L, Goosens A, Olson DJH, Ross AR, Covello PS.* The molecular cloning of artemisinic aldehyde Delta11(13) reductase and its role in glandular trichome-dependent biosynthesis of artemisinin in *Artemisia annua*. J Biol Chem 2008; 283: 21 501–21 508
12 *Teoh KH, Polichuk DR, Reed DW, Covello PS.* Molecular cloning of an aldehyde dehydrogenase implicated in artemisinin biosynthesis in *Artemisia annua*. Botany 2009; 87: 635–642
13 *Koda Y.* The role of jasmonic acid and related compounds in the regulation of plant development. Int Rev Cytol 1992; 135: 155–199
14 *Creelman RA, Mullet JE.* Biosynthesis and action of jasmonates in plants. Plant Mol Biol 1997; 48: 355–381
15 *Sy L, Brown GD.* The mechanism of the spontaneous autoxidation of dihydroartemisinic acid. Tetrahedron 2002; 58: 897–908
16 *Mueller MJ, Brodschelm W, Spannagl E, Zenk MH.* Signaling in the elicitation process is mediated through the octadecanoid pathway leading to jasmonic acid. Proc Natl Acad Sci USA 1993; 90: 7490–7494
17 *Gundlach H, Müller MJ, Kutchan TM, Zenk MH.* Jasmonic acid is a signal transducer in elicitor-induced plant cell cultures. Proc Natl Acad Sci USA 1992; 89: 2389–2393
18 *Baldi A, Dixit V.* Yield enhancement strategies for artemisinin production by suspension cultures of *Artemisia annua*. Bioresour Technol 2008; 99: 4609–4614
19 *De Vos RC, Moco S, Lommen A, Keurentjes JJB, Bino RJ, Hall RD.* Untargeted large-scale plant metabolomics using liquid chromatography coupled to mass spectrometry. Nat Protoc 2007; 2: 778–791

20 *Sasaki Y, Asamizu E, Shibata D, Nakamura Y, Kaneko T, Awai K, Amagai M, Kuwata C, Tsugane T, Masuda T, Shimada H, Takamiya K, Ohta K, Tabata S.* Monitoring of methyl jasmonate-responsive genes in *Arabidopsis* by cDNA macroarray: self-activation of jasmonic acid biosynthesis and crosstalk with other phytohormone signaling pathways. DNA Res 2001; 8: 153–161
21 *Wallaart TE, Pras N, Beekman AC, Quax WJ.* Seasonal variation of artemisinin and its biosynthetic precursors in plants of *Artemisia annua* of different geographical origin: proof for the existence of chemotypes. Planta Med 2000; 66: 57–62
22 *Cheng A, Xiang CY, Li JX, Yang CQ, Hu WL, Wang LJ, Lou YG, Chen XY.* The rice (E)-beta-caryophyllene synthase (OsTPS3) accounts for the major inducible volatile sesquiterpenes. Phytochemistry 2007; 68: 1632–1641
23 *Aguilera Y, Dorado ME, Prada FA, Martínez JJ, Quesada A, Ruiz-Gutiérrez V.* The protective role of squalene in alcohol damage in the chick embryo retina. Exp Eye Res 2005; 80: 535–543
24 *Ro D, Paradise EM, Ouellet M, Fisher KJ, Newman KL, Ndungu JM, Ho KA, Eachus RA, Ham TS, Kirby J, Chang MCY, Withers ST, Shiba Y, Sarpong R, Keasling JD.* Production of the antimalarial drug precursor artemisinic acid in engineered yeast. Nature 2006; 440: 940–943
25 *Koopmann E, Hahlbrock K.* Differentially regulated NADPH: cytochrome P450 oxidoreductases in parsley. Proc Natl Acad Sci USA 1997; 94: 14954–14959
26 *Mizutani M, Ohta D.* Two isoforms of NADPH : cytochrome P450 reductase in *Arabidopsis thaliana*. Gene structure, heterologous expression in insect cells, and differential regulation. Plant Physiol 1998; 116: 357–367
27 *Kirch HH, Dorothea B, Wei Y, Schnable PS, Wood AJ.* The ALDH gene superfamily of *Arabidopsis*. Trends Plant Sci 2004; 9: 371–377